



HAL
open science

Abundance of Primordial Black Holes Depends on the Shape of the Inflationary Power Spectrum

Cristiano Germani, Ilia Musco

► **To cite this version:**

Cristiano Germani, Ilia Musco. Abundance of Primordial Black Holes Depends on the Shape of the Inflationary Power Spectrum. *Physical Review Letters*, 2019, 122 (14), pp.141302. 10.1103/PhysRevLett.122.141302 . hal-01801847

HAL Id: hal-01801847

<https://hal.science/hal-01801847>

Submitted on 12 May 2022

HAL is a multi-disciplinary open access archive for the deposit and dissemination of scientific research documents, whether they are published or not. The documents may come from teaching and research institutions in France or abroad, or from public or private research centers.

L'archive ouverte pluridisciplinaire **HAL**, est destinée au dépôt et à la diffusion de documents scientifiques de niveau recherche, publiés ou non, émanant des établissements d'enseignement et de recherche français ou étrangers, des laboratoires publics ou privés.

Abundance of Primordial Black Holes Depends on the Shape of the Inflationary Power Spectrum

Cristiano Germani^{1,2,*} and Ilia Musco^{2,3,†}

¹*Departament de Física Quàntica i Astrofísica, Universitat de Barcelona, Martí i Franquès 1, 08028 Barcelona, Spain*

²*Institut de Ciències del Cosmos, Universitat de Barcelona, Martí i Franquès 1, 08028 Barcelona, Spain*

³*LUTH, UMR 8102 CNRS, Observatoire de Paris, PSL Research University, Université Paris Diderot, 92190 Meudon, France*



(Received 1 June 2018; revised manuscript received 11 February 2019; published 10 April 2019)

In this Letter, combining peak theory and the numerical analysis of gravitational collapse in the radiation dominated era, we show that the abundance of primordial black holes, generated by an enhancement in the inflationary power spectrum, is extremely dependent on the shape of the peak. Given the amplitude of the power spectrum, we show that the density of primordial black holes generated from a narrow peak is exponentially smaller than in the case of a broad peak. Specifically, for a top-hat profile of the power spectrum in Fourier space, we find that to have primordial black holes comprising all of the dark matter, one would only need a power spectrum amplitude an order of magnitude smaller than suggested previously, whereas in the case of a narrow peak, one would instead need a much larger power spectrum amplitude, which in many cases would invalidate the perturbative analysis of cosmological perturbations. Finally, we show that, although critical collapse gives a broad mass spectrum, the density of primordial black holes formed is dominated by masses roughly equal to the cosmological horizon mass measured at horizon crossing.

DOI: [10.1103/PhysRevLett.122.141302](https://doi.org/10.1103/PhysRevLett.122.141302)

Introduction.—The combination of direct and indirect constraints (for the latest results see [1–3]) indicated that primordial black holes (PBHs) could account for all of the dark matter (DM) in the approximate range $[10^{-16}, 10^{-14}] \cup [10^{-13}, 10^{-11}] M_{\odot}$.

The observational absence of isocurvature perturbations and non-Gaussianities in the latest cosmic microwave background data (CMB spectrum) favors single field models of inflation [4]. In this context it has been proposed by [5] (see also [6,7]) that a flattening of the inflationary potential, after the generation of the observed CMB spectra, might greatly enhance the power spectrum at scales smaller than those associated with the CMB so as to generate a non-negligible abundance of PBHs.

While PBHs could form by the collapse of statistical fluctuations of curvature perturbations generated during inflation, the usual slow-roll approximation, which well describes CMB physics, fails in this case [7], so that a more careful analysis must be performed, as discussed recently in [8–10]. Additionally, the abundance of PBHs depends on the amplitude of the inflationary power spectrum and a threshold \mathcal{P}_c . This threshold is related to the minimum amplitude of initial curvature perturbations eventually collapsing to form black holes.

Recently there has been some confusion about the correct estimate of \mathcal{P}_c : for example, in [5,11] a rather small value of $\mathcal{P}_c \sim \mathcal{O}(10^{-1})$ has been mistakenly equated to the analytical estimate of the critical value δ_c for the integrated density perturbations [12]. A larger value of $\mathcal{P}_c \sim \mathcal{O}(1)$ [8] was obtained by incorrectly converting the

critical amplitude of the integrated density perturbations into \mathcal{P}_c , as in [10] (in the realm of effective field theories) and in [13] (within explicit string theory realizations).

In the present letter, we show using peak theory [14] that all previous estimates of \mathcal{P}_c are actually inconsistent with the numerical simulations of PBH formation [15–19], whether or not the PBHs comprise the whole of the DM. The key point is that the threshold \mathcal{P}_c is not universal but instead strongly depends on the shape of the inflationary power spectrum.

Peak theory was already used in [20] to calculate the abundance of PBHs, without considering the relation between the shape of the inflationary power spectrum and the threshold of the energy density peak. In the following we propose an improved procedure for calculating the PBH abundance taking into account also the effect of the shape of the power spectrum.

Cosmological perturbations and PBH formation.—In the radiation dominated era, PBHs could be formed by sufficiently large cosmological perturbations collapsing after reentering the cosmological horizon. Assuming spherical symmetry, such regions can be described by the following approximate form of the metric at super-horizon scales,

$$ds^2 \simeq -dt^2 + a^2(t)e^{2\mathcal{R}(r)}[dr^2 + r^2 d\Omega^2], \quad (1)$$

where $a(t)$ is the scale factor while $\mathcal{R}(r)$ is the comoving curvature perturbation. In this regime the curvature perturbation is nonlinearly conserved [21] and, from the

Einstein equations, in the gradient expansion approximation [19,22], one has

$$\frac{\delta\rho}{\rho_b}(r, t) \simeq -\frac{1}{a^2 H^2} \frac{8}{9} e^{-5\mathcal{R}(r)/2} \nabla^2 e^{\mathcal{R}(r)/2}, \quad (2)$$

where ∇^2 is the flat space Laplacian, $H \equiv \dot{a}(t)/a(t)$ is the Hubble parameter and $\rho_b(t) = 3M_p^2 H^2(t)$ is the background energy density.

In the metric (1) the areal radius is given by $R(r, t) = a(t)r e^{\zeta(r)}$ and the amplitude of a cosmological perturbation can then be measured by the mass excess within a spherical region of radius R as

$$\frac{\delta M}{M_b} \simeq \delta(r, t) \equiv \frac{1}{V_b} \int_0^r 4\pi \frac{\delta\rho}{\rho_b} R^2 R' dr, \quad (3)$$

where $M_b(r, t) = V_b(r, t)\rho_b(t)$ is the background mass within the spherical volume $V_b(r, t) = 4\pi R^3(r, t)/3$.

As explained in [19], a PBH can be formed when the maximum of the compaction function $\mathcal{C} \equiv 2G\delta M(r, t)/R(r, t)$ is larger than a certain threshold value. This prevents the overdensity bouncing back into the expanding Universe. At superhorizon scales, when the maximum of \mathcal{C} is located well outside the cosmological horizon, this quantity is conserved and is related to the mass excess by

$$\delta(r, t) \simeq \left(\frac{1}{aHr}\right)^2 \mathcal{C}(r). \quad (4)$$

The location of this maximum, called r_m , is an important quantity measuring the characteristic scale of the density perturbation. Comparing different profiles in terms of r/r_m one has that similar shapes measured in these units have similar values of the mass excess threshold $\delta_c \equiv \delta_c(t_m, r_m)$, where t_m is defined by $a(t_m)H(t_m)r_m = 1$. This identifies the so-called horizon crossing measured in real space, but one should bear in mind that δ_c is calculated using the approximation of $\delta(r, t)$ at superhorizon scales.

Although the threshold δ_c characterizes the mass excess needed to form PBHs, it is the critical value of the peak $\delta\rho_c(0)/\rho_b$ that plays a crucial role for computing their cosmological abundance as we see in the next section.

By performing a detailed numerical study it has been found that, depending on the initial profile of the energy density, the threshold δ_c is in the range $0.41 \lesssim \delta_c \leq 2/3$, which is related to the range of critical values of the energy density calculated at the center of the overdensity, with $\delta\rho_c(0)/\rho_b \geq 2/3$ (see [19] for more details).

Applications of peak theory.—*The average density profile* In the previous section we have discussed the conditions for which a single perturbation is able to form a PBH. In this section we apply this knowledge to the cosmological perturbations generated during inflation.

Cosmological perturbations are of quantum origin and therefore their shapes and amplitudes are statistically distributed. In particular $\Delta \equiv \delta\rho/\rho_b$ is a statistical variable and since we assume that perturbation theory applies during inflation, the mean value of Δ , and thus the gradient of \mathcal{R} and its amplitude, is very small. As discussed earlier, however, to form PBHs we do need large, i.e., nonlinear, values of Δ . Therefore, we need to search for large perturbations (peaks) away from the mean value. [Because the formation of a PBH is a rare event, in principle the abundance of PBHs can be modified by non-Gaussian contributions to the statistics of the primordial curvature perturbations [23,24]. Whether or not these non-Gaussianities are important is a model dependent question that is still under debate (for more details see [23,25–27]) and is not addressed in this Letter.] Assuming that both Δ and \mathcal{R} are approximately Gaussian variables, with the help of peak theory [14], those peaks will be described only by the variance of Δ , which is completely dominated by the two-point function of \mathcal{R} via the linearized relation

$$\frac{\delta\rho}{\rho_b} \simeq -\frac{1}{a^2 H^2} \frac{4}{9} \nabla^2 \mathcal{R}. \quad (5)$$

Higher correlators are then suppressed by higher powers of the power spectrum of \mathcal{R} . (In a paper that appeared on the same day as ours [28], these corrections were evaluated finding that the variance of Δ is slightly larger than the one found here.) In Fourier space we then have

$$(2\pi)^3 P_\Delta(k, t) \delta(k, k') \equiv \langle \Delta(k, t) \Delta(k', t) \rangle \simeq \left(\frac{k}{aH}\right)^4 \frac{16}{81} \times (2\pi)^3 \delta(k+k') \frac{2\pi^2 \mathcal{P}(k)}{k^3}, \quad (6)$$

where we have used a standard definition of the curvature perturbation power spectrum $\mathcal{P}(k)$ [29]. Finally, we can then define the moments of $P_\Delta(k, t)$ as

$$\sigma_j^2(t) \equiv \int \frac{k^2 dk}{2\pi^2} P_\Delta(k, t) k^{2j}. \quad (7)$$

The density of PBHs at the moment of formation must be much smaller than the density of the background radiation, otherwise they will dominate the present Universe when it becomes matter dominated. For this reason the peaks generating PBHs must be rare and, to a good approximation, can be considered spherical. Nonsphericity of the peaks would be obtained by the interaction of different adjacent overdensities [14].

The observed superhorizon density profile is constructed by using the multivariate Gaussian distribution of the (real space) random field $\Delta(r, t)$. Following [14] the superhorizon averaged density profile is measured in terms of the

relative amplitude of the peak defined as $\nu \equiv [\mathcal{F}(0)/\tilde{\sigma}_0] \gg 1$, which implies that peaks are rare. Then the mean overdensity profile per given central value is

$$F(r, t) \simeq \frac{\mathcal{F}(r)}{a^2 H^2}, \quad (8)$$

with

$$\mathcal{F}(r) \equiv \mathcal{F}(0) \frac{\xi(r, t)}{\xi(0, t)}, \quad (9)$$

where $\tilde{\sigma}_0 \equiv \sigma_0(t) a^2 H^2$ and $\mathcal{F}(0)/(aH)^2$ is the amplitude of the overdensity at the center of the profile and

$$\xi(r, t) = \frac{1}{2\pi^2 \times (2\pi)^3} \int dk k^2 \frac{\sin(kr)}{kr} P_\Delta(k, t). \quad (10)$$

In this limit the number density of peaks corresponding to a given amplitude $\mathcal{F}(0)$, in the comoving volume, is

$$\mathcal{N}_c(\nu) = \frac{k_*^3}{4\pi^2} \nu^3 e^{-\nu^2/2} \theta(\nu - \nu_c), \quad (11)$$

where $k_* \equiv (\sigma_1/\sqrt{3}\sigma_0)$ and, at superhorizon scales, ν is time independent. The critical value ν_c discriminates between perturbations forming black holes ($\nu > \nu_c$) and perturbations dispersing into the expanding Universe ($\nu < \nu_c$). (The spreading of the profiles can be estimated following Sec. VII of [14],

$$\frac{\sqrt{\langle [\Delta(r, t_m) - \mathcal{F}(r) r_m^2]^2 \rangle}}{\mathcal{F}(r) r_m^2} \simeq \frac{1}{\nu} \frac{\sqrt{1 - \psi(r)}}{\psi(r)},$$

where $\psi(r) \equiv [\xi(r, t)/\xi(0, t)]$. Since $\nu \gg 1$ our approximation of considering only the threshold value of the mean profile, instead of the mean threshold, is a good one around the peak. There would be some small effects related to the edge of the profile, but since they are small for the calculation of the threshold [19], we neglect them here (for more details we refer to [28] where these effects have been estimated).

Abundance and mass spectrum of PBHs The number of sufficiently large peaks at superhorizon scales gives us the number of PBHs formed once the overdensity crosses the horizon. Then the number density of PBHs in physical space, at the moment of formation, is given by

$$\mathcal{N}_p(\nu) = \frac{\mathcal{N}_c(\nu)}{a(t_f)^3},$$

where t_f is the time when the PBHs are formed. Note that k_*/a is not dependent on the rescaling of the scale factor and so the same is also valid for $\mathcal{N}_p(\nu)$, as it should be. Finally, we are now able to define the density of PBHs of a given mass $M_{\text{PBH}}(\nu)$ at formation to be

$$\rho_{\text{PBH}}(\nu) \simeq M_{\text{PBH}}(\nu) \mathcal{N}_p(\nu). \quad (12)$$

The relative density of PBHs that would still exist today, measured at formation with respect to the background energy density, is

$$\beta_f \equiv \int_{\nu_{\min}}^{\infty} \frac{\rho_{\text{PBH}}(\nu)}{\rho_b(t_f)} d\nu, \quad (13)$$

where $\rho_b(t_f) = 3M_p^2 H^2(t_f)$ and M_p is the Planck mass. The lower limit ν_{\min} corresponds to $M_{\min} \sim 10^{15}$ g, which is the mass of PBHs that would already have evaporated by now. To match the abundance of PBHs with the observed DM, one should have $\beta_f \simeq 10^{-8} \sqrt{M_{\text{PBH}}/M_\odot}$, as can be seen for example in [13].

For given ν , the PBH mass is well approximated by the scaling law for critical collapse [15,17],

$$M_{\text{PBH}} \simeq \mathcal{K} M_H(t_m) \left(\frac{\tilde{\sigma}_0}{a_m^2 H_m^2} \right)^\gamma (\nu - \nu_c)^\gamma, \quad (14)$$

where for radiation $\gamma \simeq 0.36$, $\mathcal{K} \sim \mathcal{O}(1)$ is a numerical coefficient that depends on the specific density profile and $M_H(t_m) \equiv 4\pi(M_p^2/H_m)$ is the horizon mass measured at horizon crossing.

Finally we have

$$\beta_f \simeq \frac{\mathcal{K}}{3\pi} \left(\frac{k_*}{a_m H_m} \right)^3 \left(\frac{\tilde{\sigma}_0}{a_m^2 H_m^2} \right)^\gamma \nu_c^{3+\gamma} \mathcal{I}(x_{\min}), \quad (15)$$

where

$$\mathcal{I}(x_{\min}) \equiv \int_{x_{\min}}^{\infty} \frac{a_f}{a_m} x^3 (x-1)^\gamma e^{-\frac{x^2}{2\nu_c^2}} dx,$$

and $x \equiv (\nu/\nu_c)$. Numerical simulations show that a_f is only weakly dependent on ν [19], giving approximately $a_f/a_m \simeq 3$, and therefore we take this factor out from \mathcal{I} .

Assuming that the horizon mass at formation is much larger than 10^{15} g, since otherwise no relevant PBH abundance would be generated (we are envisaging here that these PBHs would account for all the DM, or for a significant part of it), in the large ν_c limit, one can approximate the previous integral with its saddle point at $\nu_s \simeq \nu_c + (\gamma/\nu_c)$ as was done in [30], obtaining

$$\beta_f \simeq \sqrt{\frac{2}{\pi}} \mathcal{K} \left(\frac{k_*}{a_m H_m} \right)^3 \left(\frac{\tilde{\sigma}_0}{a_m^2 H_m^2} \right)^\gamma \nu_c^{1-\gamma} \gamma^{\gamma+1/2} e^{-\frac{\nu_c^2}{2}}. \quad (16)$$

The error from using this approximation grows slowly with ν_c but always stays around 10%, for $\nu_c = \mathcal{O}(10)$.

If the linear approximation applies ($\nu_c \gg 1$), the density of PBHs would be typically peaked at the saddle point of (15), which, inserting it into (14), gives

$$M_{\text{PBH}}(\nu_s) = 4\pi\mathcal{K} \frac{M_p^2}{H_m} \left(\frac{\tilde{\sigma}_0}{\alpha_m^2 H_m^2} \right)^\gamma \left(\frac{\gamma}{\nu_c} \right)^\gamma. \quad (17)$$

Although $M_{\text{PBH}}(\nu_s)$ still gives the right order of magnitude for the black hole masses dominating the DM density, the square root of the variance of (11) is numerically calculated to be about $1.2M_{\text{PBH}}(\nu_s)$.

Threshold of the primordial power spectrum We have so far discussed how to relate the abundance of PBHs to the primordial power spectrum in the case of rare peaks, $\nu_c \gg 1$. We see that generically $\nu_c^2 \propto \mathcal{P}^{-1}$, and so the approximation of rare peaks, implying spherical symmetry, is intimately related to the linearity of the mean primordial perturbations. In the following, as benchmarks of power spectra generated during inflation, we consider the case of a narrow power spectrum, and the opposite case of a broad spectrum, simplified as a top-hat distribution.

Narrow power spectrum The first power spectrum that we consider is

$$\mathcal{P} = \mathcal{P}_0 e^{-\frac{(k-k_p)^2}{2\sigma_p^2}}, \quad (18)$$

in the limit of $k_p^2 \gg \sigma_p^2$. In this case one obtains the critical density profile plotted with a solid line in the left panel of Fig. 1. The parameters related to this profile are $k_* \simeq \sqrt{3}k_p$, $r_m \simeq (2.74/k_p)$, and $\tilde{\sigma}_0 \simeq 0.7\sqrt{\mathcal{P}_0\sigma_pk_p^3}$. Numerical simulations give the following critical values: $\delta_c \simeq 0.51$, $\delta\rho_c/\rho_b \simeq 1.2$, $\mathcal{F}_c(0) \simeq 1.2/r_m^2 \simeq 0.16k_p^2$, which finally gives $\nu_c \simeq 0.22\sqrt{(k_p/\sigma_p\mathcal{P}_0)}$.

To compare with previous literature and give an order of magnitude estimate, we can crudely approximate $\beta_f \sim e^{-\nu_c^2/2}$. For all of the dark matter being in PBHs of

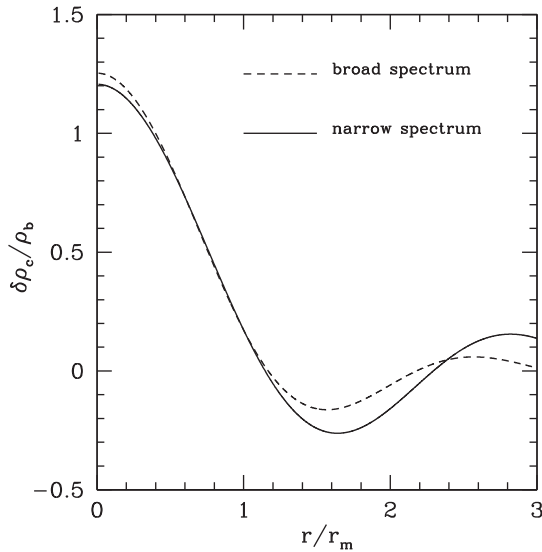


FIG. 1. This panel shows the critical density profile obtained from the narrow and broad power spectrum plotted against r/r_m .

mass $10^{-16} M_\odot$, we would need $\beta_f \sim 10^{-16}$ and therefore $\mathcal{P}_0 \sim 7 \times 10^{-4} (k_p/\sigma_p) \gg 10^{-3}$ (this does not change significantly even up to $M_{\text{PBH}} \sim 100 M_\odot$). Since for producing the seeds of PBHs from inflation one requires $\mathcal{P}_0 \ll 1$, there is only a small margin for this kind of spectrum to work.

Finally, using (17), the PBHs formed by this spectrum are peaked at $M_{\text{PBH}} \sim 0.8M_H(t_m)$.

Broad power spectrum The second power spectrum considered is a top hat with amplitude \mathcal{P}_0 , extended between $[k_{\min}$ and $k_{\max}]$, with $k_{\max} \gg k_{\min}$. (Note that modes entering the cosmological horizon much later than the formation of the apparent horizon, which typically happens at the time $t_c \sim 10t_m$ [19], will not participate in the black hole formation.) In this case, one obtains the critical density profile plotted with a dashed line in the left panel of Fig. 1 with $k_* \simeq \sqrt{2}k_{\max}$, $r_m \simeq 3.5/k_{\max}$, and $\tilde{\sigma}_0 \simeq 0.22\sqrt{\mathcal{P}_0}k_{\max}^2$.

As one can see, the two profiles in units of r/r_m are almost the same within a sphere of radius r_m . Therefore, numerical simulations give basically the same values of δ_c , $\delta\rho_c/\rho_b$ as in the previous case [19]. In terms of k_{\max} one then obtains $\mathcal{F}_c(0) \simeq 0.10k_{\max}^2$, which finally gives $\nu_c \simeq 0.46(\mathcal{P}_0)^{-1/2}$. For $\beta_f \sim 10^{-16}$ we get $\mathcal{P}_0 \sim 3 \times 10^{-3}$, one order of magnitude smaller than the value $\sim 2 \times 10^{-2}$ previously quoted in the literature, e.g., [8,10,13]. Therefore, for inflationary models generating this spectrum, it is found that PBHs are more likely to be produced than had been previously suggested in the literature.

Finally, using (17), the PBHs formed by this spectrum are peaked at a mass $M_{\text{PBH}} \sim 0.7M_H(t_m)$.

Discussion Although the expression for β_f derived in Eq. (15) differs in many aspects from the one used in the Press-Schechter approach, previously used in the literature (see e.g., [30]), the main numerical difference comes from the discordant definitions of ν_c : the PBH abundance was incorrectly related to the critical value of δ calculated at the edge of the overdensity r_0 ignoring the profile dependence of the overdensity. In particular, $\delta_0 \simeq 0.45$ corresponding to a Mexican-hat profile [17] was used earlier giving

$$\nu_0 \simeq \frac{9}{4} \frac{\delta_0}{\sqrt{\mathcal{P}_0}} \simeq 1.01\mathcal{P}_0^{-1/2}. \quad (19)$$

In Fig. 1 we plot the two energy density profiles, corresponding to the narrow and broad peaks of the power spectrum, as a function of r/r_m . The two shapes are not significantly different because the profiles of the peak of the power spectrum for $k > k_p$ or $k > k_{\max}$, which corresponds in real space to the region $r \lesssim r_m$, are very similar. Note that the Mexican-hat profile is very similar to the profiles drawn in Fig. 1 and so the value of $\delta_0 \simeq 0.45$ is the relevant one for the profiles studied in this letter.

In the left frame of Fig. 2 we plot the ratio between ν_c for the narrow and broad peak of the power spectrum

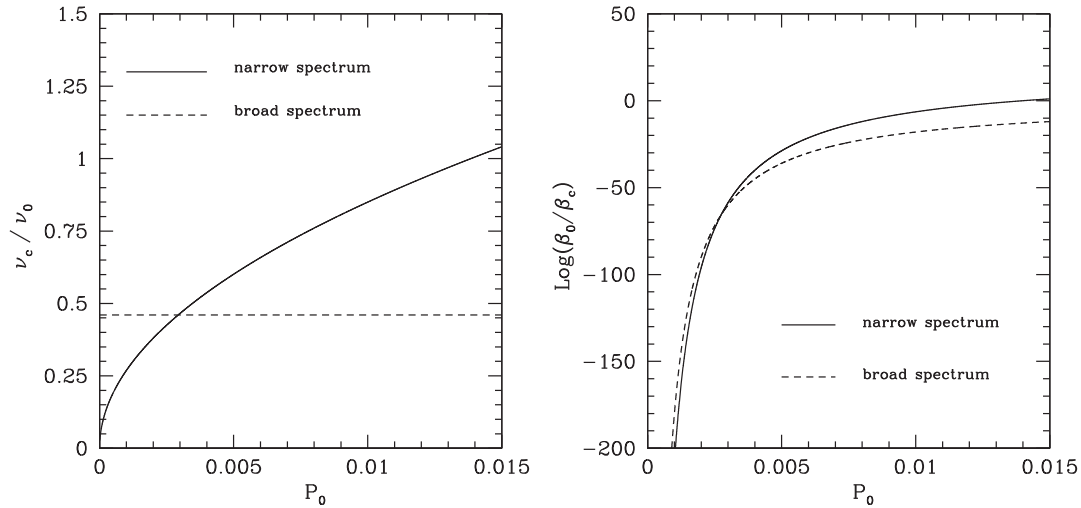


FIG. 2. The left panel shows the comparison between the threshold value ν_c and the value of ν_0 calculated previously by the use of the Press-Schechter formalism, as a function of \mathcal{P}_0 . The right panel shows instead the corresponding comparison between the approximated abundance of PBHs $\beta_c \equiv \beta(\nu_c)$ and $\beta_0 \equiv \beta(\nu_0)$. For the broad spectrum the abundance is not fixed, while for the peaked one the ratio $k_p/\sigma_{\mathcal{P}}$ has been fixed by considering $M_{\text{PBH}} \sim 10^{-16} M_{\odot}$.

calculated here with peak theory, and ν_0 given by (19) as a function of \mathcal{P}_0 , while in the right frame of Fig. 2 we plot the ratio of the corresponding relative abundance β_c/β_0 , with respect to the value of \mathcal{P}_0 . For the narrow spectrum of both plots we have fixed the abundance $\beta_f \sim 10^{-16}$ in the approximation $\beta_f(x) \sim e^{-x^2/2}$ because ν_c depends on $k_p/\sigma_{\mathcal{P}}$ and \mathcal{P}_0 , while for the broad spectrum ν_c is only a function of \mathcal{P}_0 and the abundance is therefore varying with \mathcal{P}_0 along the dashed line. The intersection between the dashed line and the solid line gives the value of \mathcal{P}_0 for the broad spectrum when $\beta_f \sim 10^{-16}$.

These plots show clearly that the approach used previously was incorrect, with a value of $\nu_c \simeq 0.5\nu_0$ for the broad spectrum, while the difference for the narrow spectrum depends on $\mathcal{P}_0 = \mathcal{P}_0(\beta_f, k_p/\sigma_{\mathcal{P}})$. The error caused by using ν_0 instead of ν_c , once the variance of the spectrum is fixed, becomes smaller for larger masses of PBHs because a larger value of β_f corresponds to a larger value of \mathcal{P}_0 . In particular, for the broad spectrum we have $\log(\beta_0/\beta_c) \simeq -2\nu_c$ which, for $M_{\text{PBH}} \sim 10^{-16} M_{\odot}$, gives $[\beta(\nu_0)/\beta(\nu_c)] \sim 10^{-64}$ (see Fig. 2) while considering for example $M_{\text{PBH}} \sim 100 M_{\odot}$, one has $[\beta(\nu_0)/\beta(\nu_c)] \sim 10^{-28}$.

Finally, let us stress that the cosmological horizon mass defined in our letter is defined at the horizon crossing time $a(t_m)H(t_m)r_m = 1$. This mass generically differs from the one used in the literature, which is calculated at the horizon crossing $a(t_k)H(t_k)/k = 1$ of a characteristic mode k (typically the one associated with the peak of the power spectrum). For example in the narrow spectrum $k = k_p$ and the mass calculated at r_m is about ten times larger than the one calculated at $1/k_p$, as was also noted in [28].

Summary.—In the present Letter we have reanalyzed the physics of PBH formation by combining peak theory [14]

with the numerical analysis of gravitational collapse in the expanding Universe [19]. We have computed the abundance of PBHs generated by a large peak in the primordial power spectrum of curvature perturbations. Characterizing the peak by its scale, amplitude, and width, we have shown that the abundance of PBHs is extremely dependent on the shape of the peak. The reason is that the threshold of the energy density peak for PBH formation depends strongly on the distribution of the real space overdensity, which can be obtained, assuming Gaussian statistics, from the two-point correlation function of curvature perturbations. This crucial aspect had been overlooked in previous literature.

Given the amplitude of the peak in the power spectrum at a particular scale, the abundance of PBHs generated by a narrow peak is exponentially smaller than the abundance generated by a broad one. In particular, to describe all of the dark matter with PBHs, using a top-hat profile of the peak in the power spectrum in Fourier space, the amplitude is an order of magnitude smaller than that previously calculated without taking into account the shape. Instead, for a narrow peak, as often assumed in the literature, one would need a much larger amplitude, which in many cases would invalidate the perturbative analysis of cosmological curvature perturbations.

Our analysis has been done assuming negligible non-Gaussianities in the initial conditions of the overdensity field. However, in certain cases, non-Gaussianities of the curvature perturbations [23] and/or non-Gaussianities related to the nonlinear relation between the curvature and overdensity perturbations [24] might give interesting contributions in the calculation of abundances of PBHs, both in terms of new statistics and for nonspherical deformations of the primordial perturbations. We leave these interesting questions for future research.

C. G. thanks Pierstefano Corasaniti and Licia Verde for discussions about peak theory and Vicente Atal for discussion about different inflationary models. I. M. thanks Misao Sasaki for discussions during the YITP long-term workshop “Gravity and cosmology,” Grant No. YITP-T-17-02. The authors thank Jaume Garriga, Juan Garcia-Bellido, and John Miller for feedback and comments on the previous version of this letter. C. G. is supported by the Ramon y Cajal program and partially supported by the Unidad de Excelencia María de Maeztu Grant No. MDM-2014-0369 and by the national Grants No. FPA2013-46570-C2-2-P and No. FPA2016-76005-C2-2-P. I. M. is supported by the Unidad de Excelencia María de Maeztu Grant No. MDM-2014-0369.

*germani@icc.ub.edu

†iliamusco@icc.ub.edu

- [1] A. Katz, J. Kopp, S. Sibiryakov, and W. Xue, *J. Cosmol. Astropart. Phys.* **12** (2018) 005.
- [2] B. Carr, M. Raidal, T. Tenkanen, V. Vaskonen, and H. Veermäe, *Phys. Rev. D* **96**, 023514 (2017).
- [3] M. Zumalacarregui and U. Seljak, *Phys. Rev. Lett.* **121**, 141101 (2018).
- [4] Y. Akrami *et al.* (Planck Collaboration), arXiv:1807.06211.
- [5] J. Garcia-Bellido and E. Ruiz Morales, *Phys. Dark Universe* **18**, 47 (2017).
- [6] I. Wolfson and R. Brustein, *PLoS One* **13**, 1 (2018).
- [7] K. Kannike, L. Marzola, M. Raidal, and H. Veerme, *J. Cosmol. Astropart. Phys.* **09** (2017) 020.
- [8] C. Germani and T. Prokopec, *Phys. Dark Universe* **18**, 6 (2017).
- [9] H. Motohashi and W. Hu, *Phys. Rev. D* **96**, 063503 (2017).
- [10] G. Ballesteros and M. Taoso, *Phys. Rev. D* **97**, 023501 (2018).
- [11] J. M. Ezquiaga, J. Garcia-Bellido, and E. Ruiz Morales, *Phys. Lett. B* **776**, 345 (2018).
- [12] T. Harada, C. M. Yoo, and K. Kohri, *Phys. Rev. D* **88**, 084051 (2013); **89**, 029903(E) (2014).
- [13] M. Cicoli, V. A. Diaz, and F. G. Pedro, *J. Cosmol. Astropart. Phys.* **06** (2018) 034; O. Zsoy, S. Parameswaran, G. Tasinato, and I. Zavala, *J. Cosmol. Astropart. Phys.* **07** (2018) 005.
- [14] J. M. Bardeen, J. R. Bond, N. Kaiser, and A. S. Szalay, *Astrophys. J.* **304**, 15 (1986).
- [15] J. C. Niemeyer and K. Jedamzik, *Phys. Rev. D* **59**, 124013 (1999).
- [16] M. Shibata and M. Sasaki, *Phys. Rev. D* **60**, 084002 (1999).
- [17] I. Musco, J. C. Miller, and L. Rezzolla, *Classical Quantum Gravity* **22**, 1405 (2005); A. G. Polnarev and I. Musco, *Classical Quantum Gravity* **24**, 1405 (2007); I. Musco, J. C. Miller, and A. G. Polnarev, *Classical Quantum Gravity* **26**, 235001 (2009); I. Musco and J. C. Miller, *Classical Quantum Gravity* **30**, 145009 (2013).
- [18] T. Harada, C. M. Yoo, T. Nakama, and Y. Koga, *Phys. Rev. D* **91**, 084057 (2015).
- [19] I. Musco, arXiv:1809.02127.
- [20] A. M. Green, A. R. Liddle, K. A. Malik, and M. Sasaki, *Phys. Rev. D* **70**, 041502 (2004); S. Young, C. T. Byrnes, and M. Sasaki, *J. Cosmol. Astropart. Phys.* **07** (2014) 045.
- [21] D. H. Lyth, K. A. Malik, and M. Sasaki, *J. Cosmol. Astropart. Phys.* **05** (2005) 004.
- [22] D. S. Salopek and J. R. Bond, *Phys. Rev. D* **42**, 3936 (1990); M. Shibata and M. Sasaki, *Phys. Rev. D* **60**, 084002 (1999).
- [23] V. Atal and C. Germani, *Phys. Dark Univ.* **24**, 100275 (2019).
- [24] A. Kehagias, I. Musco, and A. Riotto (in preparation).
- [25] Y. F. Cai, X. Chen, M. H. Namjoo, M. Sasaki, D. G. Wang, and Z. Wang, *J. Cosmol. Astropart. Phys.* **05** (2018) 012; G. Franciolini, A. Kehagias, S. Matarrese, and A. Riotto, *J. Cosmol. Astropart. Phys.* **03** (2018) 016.
- [26] C. Pattison, V. Vennin, H. Assadullahi, and D. Wands, *J. Cosmol. Astropart. Phys.* **10** (2017) 046; J. M. Ezquiaga and J. Garcia-Bellido, *J. Cosmol. Astropart. Phys.* **08** (2018) 018.
- [27] D. Cruces, C. Germani, and T. Prokopec, arXiv:1807.09057.
- [28] C. M. Yoo, T. Harada, J. Garriga, and K. Kohri, *Prog. Theor. Exp. Phys.* **2018**, 123 (2018).
- [29] V. Mukhanov, *Physical Foundations of Cosmology*, 1st ed. (Cambridge University Press, New York, 2005).
- [30] B. Carr, F. Kuhnel, and M. Sandstad, *Phys. Rev. D* **94**, 083504 (2016).